System Level Modeling of Electrolyzers for Digital Real-Time Applications

Nils Nemsow
Institute for Technical Physics (ITEP)
Karlsruhe Institute of Technology (KIT)
Karlsruhe, Germany
0000-0002-7630-9421

Giovanni De Carne
Institute for Technical Physics (ITEP)
Karlsruhe Institute of Technology (KIT)
Karlsruhe, Germany
0000-0002-3700-2902

Abstract—With the increasing share of renewable energies in electric power grids, the need for energy storage systems grows. Electrolysis plants provide a promising technology as energy storage for power-to-gas applications, as well as frequency control and ancillary services to the power grid.

In order to study the electrolyzers' performance and their integration into the grid, real-time modeling of whole electrolysis systems plays an important role. This paper analyses the literature already available on modeling and simulation of electrolysis cells and systems. Based on the findings in previous research, an advanced dynamic modeling approach for static and dynamic modeling of electrolysis processes is proposed. During the analysis, the interactions between the electrical, physical and chemical dimension of electrolysis modeling are explicitly stressed to compose a multidimensional model on system level.

Index Terms—hydrogen, water electrolysis, real-time modeling

I. INTRODUCTION

Germany is transforming its energy sector towards zero carbon dioxide emissions. One important part of Power-to-Gas (PtG) plants, which represent a promising technology for seasonal storage, is the electrolysis system, which is fed by the electricity grid. It has been proven already, that these systems can improve power system frequency stability as they are operated as a dynamically controlled load [8]. In order to integrate electrolysis systems into grid simulations, it is necessary to develop an accurate model covering the static behavior such as the dependency on temperature and pressure as well as the dynamic features and time constants for load changes.

II. ELECTROLYSIS TECHNOLOGY

A. Electrolyzer types

The development in technology has brought up different types of electrolysis cells, which differ in terms of the electrolyte, membrane and also the transported ions. Two of these types are at a high technological readiness level and will therefore be considered in this paper. One of them is the more mature alkaline electrolyzer, which features a $NaOH$ or KOH solution where OH^- ions are transported through a permeable membrane. On the other hand, there is the more

modern proton exchange membrane (PEM) electrolyzer, with H^+ ions being transported through a Nafion membrane, being separator and electrolyte at the same time. It has a remarkably lower time constant than the former and it can therefore better respond to dynamic load changes [16].

B. From cell to system

Due to the fact that a single cell is operated at a voltage between 1.5 V and 2 V [16], cells are connected in series to form stacks. Depending on the size of the cell and the system, one or several stacks, connected in parallel, are powered by a controllable DC power supply. The power supply is usually a grid-connected rectifier which is operated as a controlled voltage or current source to manage the power consumption and hydrogen production of the system [17].
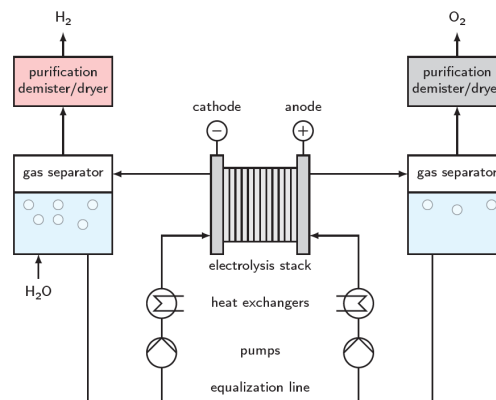

Fig. 1: Flow diagram of an alkaline electrolyzer [6]

Furthermore, the functionality of an electrolysis system is based on the constant feed-in of water (H_2O) and removal of pure hydrogen (H_2) and oxygen (O_2). This implies the need for supply pumps, as shown in Fig. 1, as well as gas drying purification units which are considered auxiliary energy consumers. Since the stack's temperature has a significant effect on its functionality and efficiency, a temperature management unit is also part of electrolysis systems. It consists of heat exchangers, re-cooling circuits and pumps letting the water or the alkaline solution circulate through the stack. The control of the thermo-managment unit ensures an almost stable stack

temperature across the whole operation range. After all, the main components of an electrolysis system are the stack, the power supply and the 'Balance of Plant' (BoP) units consisting of thermo-management and mass feed-in and feed-out.

III. STATE OF THE ART

Electrolysis systems are generally composed of the electrolysis stack itself (typically more than 100 cells in series), BoP equipment and a power supply unit. The following paragraphs give an overview of the recent approaches in modeling the whole system as well as parts of it. It is thereby distinguished between static and dynamic behavior, as both steady state and transition time constants are important to system level modeling. Electrolysis models can cover up to three dimensions. There is the electrical dimension, which is of fundamental importance to the power supply control. The chemical dimension, including the hydrogen outflow modeling, sets certain constraints to the operating point of the system. The physical dimension can be regarded as the influence of pressure and temperature on the system.

A. Static modeling

In [1,2] detailed equations are given for the relationship of voltage and current: $V = f(I)$. More specific explanation will be given in chapter IV-A. There are analytical models for PEM as well as alkaline electrolyzers in the electrical dimension only. Since these models have been investigated on cell level, neither BoP components and power supply, nor other dimensions have been considered. However, they have been tested against experimental data and proven to be slightly more accurate than previous models.

Detailed research on the hydrogen production rate and efficiency depending on the power input is presented in [5]. A multidimensional system level study is provided in [15], it investigates the influence of the operation profile on temperature and pressure in the system, and vice versa, to suggest the optimal membrane thickness and temperature and pressure level. This work also includes verification of the model by several experiments. However, the electrical dimension is understudied, there is no information on the dynamic properties of the system. Concerning the power supply units for electrolysis systems, [17] gives an overview of state-of-the-art power converter systems and future solutions to supply water electrolyzers.

B. Dynamic modeling

Covering the physical and the electrical dimension, [10] investigates a combined steady-state electrical and dynamic thermal model of a PEM electrolysis system. A similar approach, with experimental validation and a dynamic hydrogen production sub-model, can be found in [7]. Experimental studies on the electrical dynamic characteristic of an alkaline electrolyzer are conducted in [14], where also the dependency on the temperature is explicitly stressed. A complete one-dimensional dynamic model on system level has been presented in [9] showing the chemical dimension only. It

features relatively high time constants of the changes in water concentration and temperature following a change in the stack current. Multidimensional modeling on system level, with special focus on the physical dimension, is presented in [12]. It has been developed using the Bond Graph method and follows a multiphysics system modeling approach to investigate the dynamic properties of the system with a time step of 1 s.

TABLE I: State of the art

	Static cell	Static system	Dynamic cell	Dynamic system	Dynamic multidimensional
[1]	x				
[2]	x				
[5]		x			
[7]				x	
[9]				x	
[10]				x	
[12]					x
[14]			x		
[15]		x			
[17]		x			

Summarizing the state of the art in Table I, it is noticeable that only a few models take the whole system into account and there is only few literature available on multidimensional electrolysis system dynamic modeling, especially for the electrical dimension.

IV. MODEL DEVELOPMENT

The electrolysis system model can, as well as the system itself, be divided into several units which are operating independently, while still sharing common interfaces and influencing each other. Besides the simplification and easier readability of the model, the possibility of simulating the units with different time constants is a main advantage of this approach. For each sub-model, the electrical, chemical and physical dimension should be considered, as far as necessary.

Since the aim of this paper is to propose a system level model for real-time simulation, a compromise between high simulation precision on the one hand and simpleness for lower computational effort one the other hand will be outlined.

A. Cell and stack modeling

Electrolysis stacks are usually modeled as simple cells, the series connection of them is reproduced by multiplication of the parameters. This approach yields a sufficient precision for simulation, while neglecting the aging process of single cells, which can often be random. For electrolysis cell modeling in the electrical dimension, two approaches have been followed in recent research: one is building an electrical equivalent circuit out of capacitances and resistances, the other approach is to model the stack in form of a voltage source, based on electrochemical phenomena.

a) Electrical equivalent circuit: The Randles-Warburg (RW) cell, consisting of the Randles circuit and a simplified Warburg impedance, is expected to be an adequate model for the impedance of galvanic and electrolytic cells [11]. Together with the standard electrode potential V_{rev}, it provides an

equivalent circuit to model the electrical cell dynamics of an electrolysis cell. This circuit, which is composed of several resistive and capacitive elements, is shown in Fig. 2.
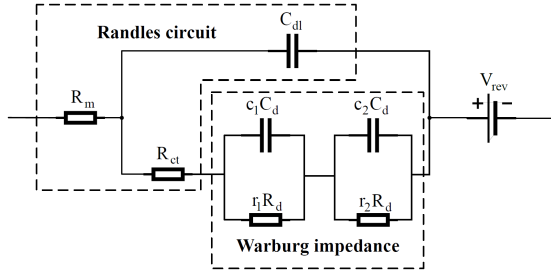

Fig. 2: Randles-Warburg equivalent circuit, adapted from [11]

In this figure, R_m represents the ohmic losses, which are mainly influenced by the membrane, C_{dl} relates to the cell's electrical double layer and R_{ct} is the charge transfer resistance representing the activation losses. The simplified Warburg impedance is considered as a model for the concentration losses within the electrolyzer. It is calculated from two RC elements accounting for anode and cathode with R_d, C_d being diffusion resistance and diffusion capacitance and r_1, c_1, r_2, c_2 being dimensionless Warburg coefficients. All of these values are considered constant parameters that can be obtained from a single cell using the current interruption method [13]. To sum up, the RW circuit is a simple but sufficient approach to model the dynamic behavior of an electrolytic cell. It is suitable for alkaline as well as PEM electrolyzers.
However, due to the fact that the parameters are fitted to match experimental data, they might be accurate for a certain range of cell current, but they are only accurate for a small range of cell temperature and pressure. The dependency of the electrical performance on physical ambient conditions is neglected in the standard Randles-Warburg equivalent circuit approach. Furthermore, there is no information available on the hydrogen production or the heat dissipation.

b) Electrochemical model: From the analytical perspective, the electrolytic cell may be modeled as a voltage source in the electrical dimension. Interdependencies with the chemical and physical dimension can be simulated using defined interfaces, for example for temperature change, power dissipation or gas concentration. The following electrochemical model has been adapted from [2] for an alkaline water electrolyzer. The voltage of the source is the sum of four overvoltages related to processes and features of the cell.

$$V = V_{oc} + V_{act} + V_{con} + V_{ohm} \tag{1}$$

In the equation (1), V_{oc} is the open-circuit voltage, V_{act} ist the activation overvoltage, V_{con} is the concentration overvoltage and V_{ohm} is the ohmic overvoltage. These four components will be explained in the following. The open-circuit (or equilibrium) voltage is lower for rising temperature and higher for rising pressure. It can be obtained from the Nernst equation:

$$V_{oc} = V_{rev} + (T - T_{ref}) \cdot \frac{\Delta S^0}{nF} + \frac{R^* T}{2F} \cdot \ln\left(\frac{p_{H_2} \cdot \sqrt{p_{O_2}}}{a_{H_2O,KOH}}\right) \tag{2}$$

$$
\begin{aligned}
V_{rev} &= & 1.229 \text{ V} \\
T_{ref} &= & 25 \text{ °C} \\
\frac{\Delta S^0}{nF} &= & -0.9 \cdot 10^{-3} \frac{\text{J}}{\text{mol·K}}
\end{aligned}
$$

This equation includes the reversible cell voltage V_{rev} and adds temperature-dependent and pressure-dependent terms. T_{ref} is the reference temperature for V_{rev} at atmospheric pressure and $\frac{\Delta S^0}{nF}$ is the standard state entropy change. R^* denotes the universal gas constant and F the Faraday constant. The partial pressures of hydrogen and oxygen p_{H_2}, p_{O_2} and the water activity in the alkaline solution $a_{H_2O,KOH}$ are influencing factors from the chemical dimension. They have been adapted from [3,4] and are influenced by the product gas pressure, the molar concentration of the alkaline solution and the temperature. The activation overvoltages of anode (3) and cathode (4) are calculated separately by adapting the Butler-Volmer equation and then summed up (5).

$$V_{act}^{an} = \frac{R^* \cdot T}{\alpha_{an} \cdot F} \cdot \ln\left(\frac{i}{i_0^{an}(1 - \Theta_{an})}\right) \tag{3}$$

$$V_{act}^{cat} = \frac{R^* \cdot T}{\alpha_{cat} \cdot F} \cdot \ln\left(\frac{i}{i_0^{cat}(1 - \Theta_{cat})}\right) \tag{4}$$

$$V_{act} = V_{act}^{an} + V_{act}^{cat} \tag{5}$$

In these equations, the parameter α is the charge transfer coefficient of the electrode, Θ is its bubble coverage modeled in the chemical dimension [2] and i_0 is the effective exchange current density. It is calculated from several cell-specific parameters and the ambient temperature as follows:

$$i_0 = \gamma_M \cdot e^{-\frac{\Delta G_C}{R^*} \cdot \left(\frac{1}{T} - \frac{1}{T_{ref}}\right)} \cdot i_{0,ref} \tag{6}$$

The concentration (or diffusion) overvoltage V_{con} is caused by a decreasing concentration of the reactants near the electrode's reactive surface due to the reactions taking place. It is mathematically described by the following equation (7) featuring the actual molar concentrations at the electrodes C_{el} and a reference value C_0 for the non-reactive state.

$$V_{con} = \frac{R^* \cdot T}{4 \cdot F} \cdot \ln\frac{C_{O_2,el}^{an}}{C_{O_2,0}^{an}} + \frac{R^* \cdot T}{2 \cdot F} \cdot \ln\frac{C_{H_2,el}^{cat}}{C_{H_2,0}^{cat}} \tag{7}$$

The molar concentration values are calculated in the chemical dimension and are directly or indirectly influenced by temperature, pressure and cell current [2].
The ohmic overvoltage V_{ohm} is a product of the cell current and its resistance. It is thereby almost only influenced by the cell's geometry and materials.

$$V_{ohm} = I \cdot R_{cell} = I \cdot (R_e + R_{el} + R_s) \tag{8}$$

The cell resistance is the sum (8) of the resistances of the electrodes R_e, the electrolyte R_{el} and the separator membrane R_s. Besides the cell's geometry and materials, the electrodes' and the electrolyte's resistance is also temperature-sensitive, and the resistance of the electrolyte increases with the bubble coverage of the electrodes. Summarizing the electrochemical modeling approach, the steady-state characteristics according to (1)-(8) are visualized in Fig. 3.
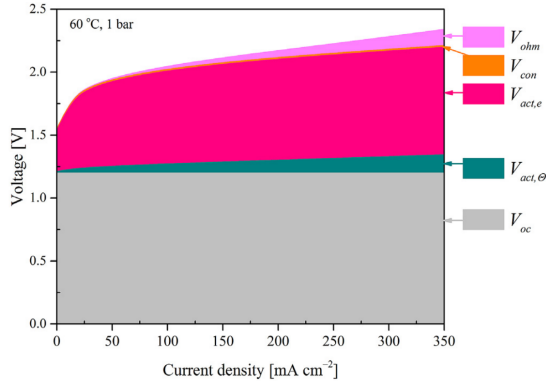
Fig. 3: Voltage-current characteristics of an alkaline cell [2]

Comparing the two presented cell and stack modeling approaches, the one-dimensional dynamic model on the one hand and the multi-dimensional static model on the other hand, a combination of both the models seems appropriate. The proposed circuit follows the electrochemical description of the alkaline electrolysis cell and is shown in Fig. 4. It features a voltage source providing the open source voltage, a Warbung impedance as well as a variable ohmic resistance. Concentration phenomena have been neglected, since they have only little impact on the cell voltage for the feasible current densities in alkaline electrolyzers.
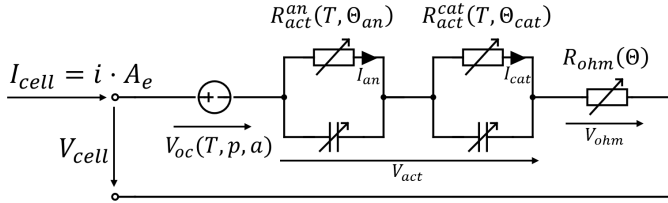

Fig. 4: Dynamic equivalent circuit approach

The equivalent circuit, which is presented here, integrates the calculations, including the dependencies, for the open-circuit voltage (2) and the ohmic overvoltage (8) from the electrochemical model [2]. The activation voltages, divided by the cell current, result in the activation resistances R_{act} used in the Warburg elements. The capacitance values are fitted to match a certain time constant. After all, a stimulation of the system by means of inflow current causes a voltage response.

B. Power supply modeling

Several requirements may be raised towards the power supply and the control of electrolyzers. On one hand, there is the DC power control following a given setpoint for hydrogen production. On the other hand, there are the grid frequency ancillary services which can also be integrated into a water electrolysis system. For power electronics modeling, there are several possibilities. Assuming that the time constants of the electrolytic cell and the period of the grid frequency are much slower than the switching period of the converters,

the state-space average model appears beneficial in terms of computational efficiency. The stack model, made of a simple multiplication of the dynamic cell equivalent circuit model, is directly connected to the converter model.

Regarding the control, a double-loop PI controller composed of an inner current controller and an outer power controller can fulfil the requirement of active power supply following a given set-point. For grid frequency support, a decoupled reactive power controller will be added to the control system.

C. Hydrogen production model

Since the production of hydrogen in an electrolysis stack is proportional to the stack current in steady state operation, its static modeling follows the equation (9) below, showing the mass flow.

$$\dot{m}_{H_2} \left[\frac{\text{kg}}{\text{h}} \right] = 1.8 \left[\frac{\text{kg} \cdot \text{s}}{\text{g} \cdot \text{h}} \right] \frac{I[\text{A}] \cdot M_{H_2} \left[\frac{\text{g}}{\text{mol}} \right]}{F \left[\frac{\text{A} \cdot \text{s}}{\text{mol}} \right]} \quad (9)$$

I is the stack current, M_{H_2} is the molar mass of hydrogen and F is the Faraday constant. For dynamic modeling, the stack current is replaced by the cathode current I_{cat} from the equivalent circuit in Fig. 4.

D. Thermal management

The temperature management of an electrolysis system can be considered as a simple controller with a large time constant to keep the stack temperature at a constant level. To do so, the fluid circulating through the stack can either be (electrically) heated or cooled down by a heat exchanger. For each electrolyzer, there is a thermoneutral point, where neither heating nor cooling power is needed [10].

E. Balance of plant modeling

BoP components in an electrolysis system are auxiliary power consumers with low dynamics. They are mostly pumps that are either in constant operation, such as the recirculation pumps for the alkaline solution, or approximately proportional to the system power, such as the pumps for the recooling circuit. Furthermore, especially for PEM electrolysis systems, there is a stack heating system, which is only active at low current densities, when the power dissipation is lower than the thermal loss.

V. MODEL ANALYSIS

For the analysis of the proposed model, realistic use cases have to be defined. These should be, as mentioned earlier, the variable production of hydrogen depending on the availability of renewable electricity and the frequency control and ancillary services to the power grid. The first scenario requires a higher-level control sending power setpoints to the electrolysis system. These setpoints are the reference value for the controller in Fig. 5, which controls the duty cycle for the buck converter powering the electrolysis stack. The second scenario is no longer realisable with a passive grid-side converter. An appropriate solution would be the IGBT based Active Front End converter with a decoupled active and
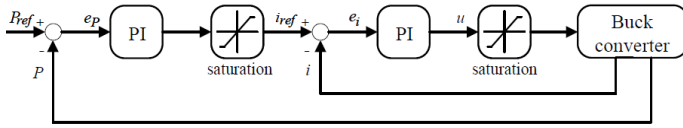
Fig. 5: Double-loop PI control for given power setpoint [18]

reactive power control. The active power control is keeping the DC-link voltage constant, the reactive power control is providing grid voltage support following the Q(U) characteristics. For the buck converter connected to the electrolysis stack, a similar control as shown in Fig. 5 can be applied, with the power reference following the P(f) characteristics for grid frequency support. In both scenarios, the electrolysis system would operate at a certain default power point, with the possibility to increase or decrease its power when needed. For further analysis, this default power point is set to 70 % of the maximum power. It is assumed that the controller requires a power decrease from 70 % to 60 % of the rated power. The reason could be a weak grid or lower availability of renewable energies. For the model analysis, a commercially available alkaline electrolysis system with a rated power of 48 kW is simulated. In this paper, only a short time period is analyzed, therefore the influence of temperature changes is not visible.

For the given power decrease scenario, the hydrogen production rate response on system level is analyzed. Reviewing the graphs in Fig. 6, it is obvious that the electrolytic stack is the element with the slowest time constant.
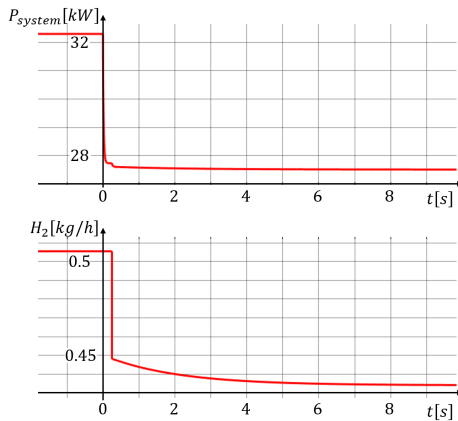

Fig. 6: power decrease and hydrogen production response

Since the lab-size electrolysis system is not operative yet, it has not been possible to validate the presented model with own experimental data. For the fitting of the parameters and the validation of the electrolysis system model, this paper relies on data already available in published literature.

VI. CONCLUSIONS

This paper presents an approach for static and dynamic modeling of electrolysis systems in a multidimensional extent. Besides the electrical behavior for given and constant ambient

conditions, this model also covers interactions with the chemical and physical dimension. Furthermore, the system level scope allows realistic experiments and the integration into a real-time smart grid simulation environment.

Further research should focus on the adjustment of the model and its parameters, especially in the physical dimension concerning heat transfer processes in the system. To optimize the slow time constants of the electrolysis system and make it more suitable for grid frequency support applications, it could be coupled with a secondary, faster energy storage system to form a hybrid energy storage plant. Together with dynamic models of storage tanks and fuel cell systems, hydrogen-based energy storage plants can be simulated in real time.

REFERENCES

[1] Z. Abdin, C. J. Webb, and E. Gray. Modelling and simulation of a proton exchange membrane (pem) electrolyser cell. *International Journal of Hydrogen Energy*, 40(39):13243–13257, 2015.
[2] Z. Abdin, C. J. Webb, and E. Gray. Modelling and simulation of an alkaline electrolyser cell. *Energy*, 138:316–331, 2017.
[3] T. Adibi, A. Sojoudi, and S. C. Saha. Modeling of thermal performance of a commercial alkaline electrolyzer supplied with various electrical currents. *International Journal of Thermofluids*, 13:100126, 2022.
[4] J. Balej. Water vapour partial pressures and water activities in potassium and sodium hydroxide solutions over wide concentration and temperature ranges. *International Journal of Hydrogen Energy*, 10(4):233–243, 1985.
[5] A. Beainy, N. Karami, and N. Moubayed. Simulink model for a pem electrolyzer based on an equivalent electrical circuit. In *International Conference on Renewable Energies for Developing Countries 2014*, pages 145–149. IEEE, 2014.
[6] J. Brauns and T. Turek. Alkaline water electrolysis powered by renewable energy: A review. *Processes*, 8(2):248, 2020.
[7] R. García-Valverde, N. Espinosa, and A. Urbina. Simple pem water electrolyser model and experimental validation. *International Journal of Hydrogen Energy*, 37(2):1927–1938, 2012.
[8] M. Kiaee, A. Cruden, D. Infield, and P. Chladek. Utilisation of alkaline electrolysers to improve power system frequency stability with a high penetration of wind power. *IET Renewable Power Generation*, 8(5):529–536, 2014.
[9] H. Kim, M. Park, and K. S. Lee. One-dimensional dynamic modeling of a high-pressure water electrolysis system for hydrogen production. *International Journal of Hydrogen Energy*, 38(6):2596–2609, 2013.
[10] M. E. Lebbal and S. Lecœuche. Identification and monitoring of a pem electrolyser based on dynamical modelling. *International Journal of Hydrogen Energy*, 34(14):5992–5999, 2009.
[11] C. A. Martinson, G. van Schoor, K. R. Uren, and D. Bessarabov. Characterisation of a pem electrolyser using the current interrupt method. *International Journal of Hydrogen Energy*, 39(36):20865–20878, 2014.
[12] P. Olivier, C. Bourasseau, and B. Bouamama. Dynamic and multiphysic pem electrolysis system modelling: A bond graph approach. *International Journal of Hydrogen Energy*, 42(22):14872–14904, 2017.
[13] M. A. Rubio, A. Urquia, and S. Dormido. Diagnosis of pem fuel cells through current interruption. *Journal of Power Sources*, 171(2):670–677, 2007.
[14] X. Shen, X. Zhang, G. Li, T. T. Lie, and L. Hong. Experimental study on the external electrical thermal and dynamic power characteristics of alkaline water electrolyzer. *International Journal of Energy Research*, 42(10):3244–3257, 2018.
[15] G. Tjarks. *PEM-Elektrolyse-Systeme zur Anwendung in Power-to-Gas Anlagen*. Phd thesis, Forschungszentrum Jülich, Jülich, 2017.
[16] J. Töpler and J. Lehmann. *Wasserstoff und Brennstoffzelle*. Springer Berlin Heidelberg, Berlin, Heidelberg, 2014.
[17] B. Yodwong, D. Guilbert, M. Phattanasak, W. Kaewmanee, M. Hinaje, and G. Vitale. Ac-dc converters for electrolyzer applications: State of the art and future challenges. *Electronics*, 9(6):912, 2020.
[18] H. Zhang. *Modeling and Analysis of A PEM Electrolysis System for Parallel Simulation*. Master's thesis, Karlsruher Institut für Technologie, 2022.